

---

# Counterfactual Explanations for Arbitrary Regression Models

---

**Thomas Spooner**

J. P. Morgan AI Research  
thomas.spooner@jpmorgan.com

**Danial Dervovic**

J. P. Morgan AI Research  
danial.dervovic@jpmorgan.com

**Jason Long**

J. P. Morgan AI Research  
jason.x.long@jpmorgan.com

**Jon Shepard**

J. P. Morgan AI Research  
jon.shepard@jpmorgan.com

**Jiahao Chen**

J. P. Morgan AI Research  
jiahao.chen@jpmorgan.com

**Daniele Magazzeni**

J. P. Morgan AI Research  
daniele.magazzeni@jpmorgan.com

## Abstract

We present a new method for counterfactual explanations (CFEs) based on Bayesian optimisation that applies to both classification and regression models. Our method is a globally convergent search algorithm with support for arbitrary regression models and constraints like feature sparsity and actionable recourse, and furthermore can answer multiple counterfactual questions in parallel while learning from previous queries. We formulate CFE search for regression models in a rigorous mathematical framework using differentiable potentials, which resolves robustness issues in threshold-based objectives. We prove that in this framework, (a) verifying the existence of counterfactuals is NP-complete; and (b) that finding instances using such potentials is CLS-complete. We describe a unified algorithm for CFEs using a specialised acquisition function that composes both expected improvement and an exponential-polynomial (EP) family with desirable properties. Our evaluation on real-world benchmark domains demonstrate high sample-efficiency and precision.

## 1 Introduction

Counterfactual explanations (CFEs) have garnered attention in the explainable AI (XAI) literature [35] as a tool for inspecting the outputs of machine learning models [53, 12, 35]. In its most basic form, a CFE of a model  $f$  takes an input *query instance*  $q$  belonging to the input data space and applies a minimal perturbation  $\varepsilon$  such that the new model output,  $f(q + \varepsilon)$ , differs from the original output,  $f(q)$ , in some desired way. The ability to inspect local changes in a model’s output allows one to understand a decision boundary in more detail, diagnose issues with robustness or to suggest ways consumers of a model’s output can improve their own model-dependent outcomes. The latter idea is known as *actionable recourse* [27, 52], and is important for high-stakes decisions such as credit decisioning and healthcare. The European Union now legally stipulates that any individual subject to (semi)-autonomous decision making has the *right* to an explanation [54, 16], and similar rights to explanation have existed in the US in domains such as credit decisioning [11].

Existing work on CFEs focus on classification models [5]. Since the model outputs are discrete, the notion of when a model’s output changes is unambiguous. In contrast, regression models have

continuous outputs which can change under arbitrarily small perturbations. Applying the usual notion of counterfactuals (CFs) to explain changes to regression models is hence prone to CFEs that are essentially uninformative by dint of their being too similar to the query instance. The naïve solution to this problem, by requiring a minimal threshold of change on the dependent variables, turns out to be very sensitive to the chosen threshold, as we describe in Section 2. This phenomenon suggests that there are questions around counterfactual specification that have yet to be addressed.

**Our contributions.** We present a new method for computing CFEs for regression models that is based on Bayesian optimisation. Our method is principled, yet flexible: it requires only black box access to the model, and supports arbitrary nonlinear constraints on feature perturbations. Our specific contributions are to:

1. Introduce a rigorous mathematical framework for specifying counterfactual search problems with regression models based on differentiable potentials and, in so doing, resolve the known robustness issues of threshold-based objectives.
2. Prove that, under this formalism, finding an optimal CF is CLS-complete [18], and that deciding CF existence more generally is NP-complete.
3. Motivate the definition of an exponential-polynomial (EP) family of potentials, explore their theoretical properties, and demonstrate their effectiveness on practical problems.
4. Provide a unified algorithm for generating counterfactuals with Bayesian optimisation and a specialised acquisition function based on a composition of expected improvement and the EP family of potential functions.

To the best of our knowledge, we are the first to use Bayesian optimisation to generate CFEs.

## 1.1 Related Work

Several comprehensive surveys on CFEs have recently been published [10, 53, 49]. CF generation techniques vary by how much we can introspect into the model. On one extreme, some methods use only black box access to model outputs, and are model agnostic [14, 42]. On the other, methods exist that require full introspection into the model’s specification, notably for tree ensembles [50, 30, 19]. Such methods are specific to a particular class of model. Intermediate between these are methods that require gradient information, which presumes that the model is differentiable [40, 38, 29].

**Computational cost.** In general, CFE methods that require fewer assumptions about the model have higher computational complexity. The CF search is often formulated as a non-convex optimisation problem, although some convexified formulations do exist [1, 2], and are computationally hard to solve optimally [34, 22]. Despite this cost, we use Bayesian optimisation (BO) for our CF search, as it is globally convergent [21, 48, 8] and is efficient in practice [47, 6]. To amortize the cost incurred in CFE search, some methods provide multiple diverse CFEs to a given query instance [38, 14, 19], while others permit reuse of a single optimisation run to generate CFEs for multiple query instances [33]. Our method is an example of the latter.

**Desiderata.** **Sparsity.** Human interpretable CFEs should involve changes to only a few features, and is usually enforced by  $\ell_1$ -regularisation [30, 19, 27, 38] or  $\ell_0$ -regularisation [14]. However, such sparsity penalties are not always appropriate, particularly when handling predictive multiplicity, when multiple trained classifiers all have similar output [56, 39]. In our method, sparsity can be induced by any  $\ell_p$ -regulariser as specified by the user. **Proximity.** Generated CFEs should be close to the manifold of observed data [14, 40, 26]. **Causality.** CFEs should account for causal relations between features [7, 27, 33], assuming the underlying causal structure is known [41]. **Actionability (recourse).** The changes described in a CFE can be realized in a future input to the model, which requires methods to distinguish between mutable and immutable features [26, 14, 27]. Our method permits nonlinear constraints, which allows the user to impose their own actionability properties; for instance, that age can only increase, or that two features must change in the same direction. **Use of categorical features.** Categorical features must be processed into a differentiable representation before they can be used in gradient-based methods. Methods like the standard Gumbel-softmax trick [23, 32] presents scaling issues when many categories are present [55]. Some methods like MiVaBo [15] and CoCaBO [45] permit Bayesian optimisation over mixed variables, while others use

Table 1: Key properties of our counterfactual generation algorithm.

|                        | Property                       | Description  | Value          |
|------------------------|--------------------------------|--|----------------|
| <i>Assumptions</i>     | Model Access<br>Model Agnostic | How much information is needed about the model?<br>Is the algorithm model-independent? | Black Box<br>✓ |
| <i>Optimisation</i>    | Amortised Inference            | CF generation for multiple query instances without optimising separately               | ✗              |
| <i>Amortisation</i>    | Multiple Counterfactuals       | Multiple CF examples produced for a given query instance                               | ✓              |
| <i>CF Attributes</i>   | Sparsity                       | Does the algorithm consider sparsity?  | ✓              |
|                        | Data Manifold                  | Are generated examples forced to be close to the data manifold?                        | ✗              |
|                        | Causal relation                | Are causal relations between features considered?                                      | ✗              |
| <i>CF Optimisation</i> | Feature preference             | Is feature actionability accounted for?  | ✓              |
| <i>Attributes</i>      | Categorical dist. func.        | Distance function for categorical features if different to continuous.                 | —              |

latent variables in the surrogate model [57]. In principle, our method permits the use of any such representation of categorical variables. In this paper, we focus on methods available in GPpyOpt [4], upon which we implement our algorithm.

Table 1 describes our method using the categorisation of Verma et al. [53], while noting that this categorisation excludes regressions. At present, the only other CFE method that is black-box, model-agnostic and capable of producing multiple counterfactual example is Dandl et al. [14]. Like us, they pose CFE as an optimisation problem. Also, the method applies to both regression and classification models, albeit focusing on the latter. Our method differs in two key aspects. First, we use *counterfactual potentials* instead of thresholding, which we argue in Section 2 is not appropriate in general. Second, we use Bayesian optimisation, which guarantees global convergences as in Theorem 3.2, instead of genetic programming, which does not provide such convergence rigorously.

## 2 Counterfactual Search and its Complexity

The generation of CFEs can be formulated as a classic search, or satisfiability problem. Given some model  $f : \mathcal{X} \rightarrow \mathcal{Y}$ , where  $\mathcal{X}$  is of finite dimensionality — but possibly infinite in cardinality — and a query instance  $q \in \mathcal{X}$ , the objective is, broadly speaking, to identify another input  $c \neq q$ ,  $c \in \mathcal{X}$ , such that the new output qualifies as “contrary to the fact”. To formalise this, we first introduce the notion of a *counterfactual algebra* which contains all possible subsets of a model’s range, excluding  $f(q)$ . We then identify a form of duality between the chosen target set and the input values that could plausibly give rise to an output in this region. These two concepts characterise the problem of finding a CFE, regardless of the domain or codomain of the model.

**Definition 2.1** (Counterfactual Algebra). For a model-query pair  $(f, q)$ , define the *counterfactual algebra* as the powerset

$$\mathbb{T}_q^f \doteq \mathcal{P}(\{f(x) : x \in \mathcal{X}, f(x) \neq f(q)\}). \quad (1)$$

Further, let  $\widetilde{\mathbb{T}}_q^f \subset \mathbb{T}_q^f$  denote the set of subsets that admit polynomial-time membership circuits/oracles (see Definition A.1).

**Definition 2.2** (Counterfactual Duality). Take a model-query pair  $(f, q)$  and choose a *target set*  $\mathcal{T} \in \mathbb{T}_q^f$  to be the *dual space*. The corresponding *primal* (or, *counterfactual*) space is then defined as the preimage of the target set under  $f$ ,

$$\mathcal{S}_{\mathcal{T}}^f \doteq f^{-1}[\mathcal{T}] = \{x \in \mathcal{X} : f(x) \in \mathcal{T}\}. \quad (2)$$

The abbreviated notations  $\mathcal{S}_{\mathcal{T}}$  and  $\mathcal{S}$  will be used when  $f$  and/or  $\mathcal{T}$  are clear from context.

The construction above makes it clear that the outcome and efficacy of any counterfactual experiment hinges on (a) the nature of the domain  $\mathcal{X}$  and codomain  $\mathcal{Y}$ ; (b) the query instance  $q \in \mathcal{X}$ ; and (c) the choice of target set  $\mathcal{T} \in \mathbb{T}_q^f$ . While Definition 2.1 implies that any element  $x \in \mathcal{T}$  is reachable under the model, it says nothing of how difficult it is to find such a point. To provide intuition into this property of CF search, we define a new computational problem CFX-EXISTENCE below and prove in Theorem 2.1 that it is NP-complete. In other words, while finding a solution may be hard, verifying CFEs for a given query instance is relatively easy.

CFX-EXISTENCE (informal)

**Input:** A model  $f : \mathcal{X} \rightarrow \mathcal{Y}$ , query  $q \in \mathcal{X}$  and target set  $\mathcal{T} \in \widetilde{\mathbb{T}}_q^f$ .

**Goal:** Decide if the counterfactual set  $\mathcal{S}$  is non-empty.

**Theorem 2.1.** CFX-EXISTENCE is NP-complete.

*Proof (Sketch).* Polynomial verification and a reduction from SAT; see Appendix A.  $\square$

Theorem 2.1 assumes that the function  $f$  is efficient to compute, which is true for many models developed in practice. For classifiers, where the set  $\mathcal{Y}$  is finite, computing set membership is trivial, and the convention is to express the target set for a given query point  $q$  as  $\mathcal{T} = \{y \in \mathcal{Y} : y \neq f(q)\}$ , or some subset thereof. Since the codomain is finite, it follows that the target set must also be finite, and thus one can construct practical algorithms that provide candidate solutions to CFX-EXISTENCE under mild constraints on the model and its domain (see Section 1.1 and references therein). In contrast, regression models have codomains that are subsets of an  $n$ -dimensional real Euclidean space, and the definition of a “valid” CF is much more nuanced. First, we may not always have an efficient algorithm for establishing whether a value is even present in the target set. Second, it is not clear how to choose a set from the model-induced algebra so as to obtain “realistic” counterfactuals.

**Setting thresholds for regression models is brittle.**

For scalar regression problems, one solution to specifying validity of CFs is to set a threshold  $\varepsilon$ , so that the CF set is  $\mathcal{S} \doteq \{x \in \mathcal{X} : |f(x) - f(q)| \geq \varepsilon\}$ . This construction yields an equivalency between instances of CFX-EXISTENCE for (binary) classifiers and regressors. They are also tractable, since the targets are defined using preorders, which admit trivial verification circuits. However, thresholding does not distinguish between CFs in  $\mathcal{S}$ , which is a problem when the distance in  $x$  far exceeds  $\varepsilon$ , leading to unrealistic CFs that are far from the query point. Furthermore, CFs defined via thresholding can be very sensitive to  $\varepsilon$ . Figure 1 shows an example where the query instance  $q \in \mathcal{X}$  is bounded above by  $q < x_1 < x_2$ , and  $f$  is monotone increasing such that  $f(q) < f(q) + \varepsilon_1 < f(x_1) < f(q) + \varepsilon_2 < f(x_2)$  for  $0 < \varepsilon_1 < \varepsilon_2$ . Define  $\Delta \doteq x_2 - x_1$ . Setting  $\varepsilon_1$  as the threshold yields the CF  $x_1$ , whereas choosing  $\varepsilon_2$  yields  $x_2$  instead. Considering the distance When  $\Delta$  is large,  $x_2$  is further from  $q$  than  $x_1$  is, and thus  $\varepsilon_2$  is arguably a worse threshold than  $\varepsilon_1$ , as it yields CFs far from the query point. However, there is no *ex ante* way to choose between  $\varepsilon_1$  and  $\varepsilon_2$ , which causes this threshold robustness issue. A key contribution our work is to formalise the notion of regression counterfactuals in terms of *potentials* instead of the direct instantiation of the primal-dual spaces via thresholds, which we will now describe.

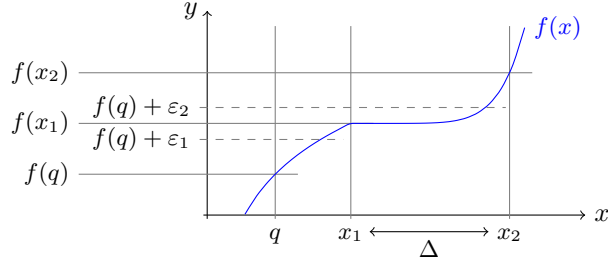


Figure 1: Threshold robustness issue with CFEs: choosing  $\varepsilon_2$  over  $\varepsilon_1$  yields  $x_2$  rather than  $x_1$  as the counterfactual.

**2.1 Potential-Based Search**

In this work, we focus on a subset of  $\mathbb{T}_q^f$  where, for a given query  $q \in \mathcal{X}$ , we ascribe to each output  $y \in \mathcal{Y}$  a scalar potential which quantifies the *value* associated with candidate counterfactual points. This concept is closely related to the construction used in potential games [37] to analyse equilibria when agents’ incentives are dictated by a single global function. Definition 2.3 below formalises this.

**Definition 2.3** (Potential). A *counterfactual potential function* is an element  $\rho$  of the set

$$\mathcal{R}_q^f \doteq \left\{ \rho \in C_L^1(\mathcal{Y}, \mathbb{R}) : \max_{x \in \mathcal{X}} \rho(f(x)) - \rho(f(q)) > 0 \right\} \quad (3)$$

of all continuously differentiable maps between model outputs and the real line, where  $(f, q)$  is a model-query pair,  $\rho$  and  $\nabla \rho$  are  $L$ -Lipschitz, and the value of  $\rho$  is not maximized at  $q$ .

Using this notion of a potential, we can now refine the counterfactual duality of Definition 2.2 into Definition 2.4 below, which naturally characterises CFs for regression models.

**Definition 2.4** (Potential Duality). For a model-query pair  $(f, q)$  and potential  $\rho \in \mathcal{R}_q^f$ , define the  $\varepsilon$ -optimal primal-dual spaces as

$$\mathcal{T}_\rho^\varepsilon \doteq \{y = f(x) : x \in \mathcal{X}, \rho(y) \geq (1 - \varepsilon)\rho^*\} \in \mathbb{T}_\rho^f \subset \mathbb{T}_q^f, \quad (4)$$

$$\mathcal{S}_\rho^\varepsilon \doteq \{x \in \mathcal{X} : f(x) \in \mathcal{T}_\rho^\varepsilon\}, \quad (5)$$

where  $\rho^* \doteq \max_{x \in \mathcal{X}} \rho(f(x))$  and  $0 \leq \varepsilon < 1$ . Let the induced sub-algebra of (potential-based) target sets be denoted by  $\mathbb{T}_\rho^f \subset \mathbb{T}_q^f$  and defined as the powerset over the  $(1 - \varepsilon)\rho^*$ -superlevel sets. As in Definition 2.1, let  $\tilde{\mathbb{T}}_\rho^f \doteq \mathbb{T}_\rho^f \cap \tilde{\mathbb{T}}_q^f$  denote the subset of efficient potential-based target sets.

*Remark.* The model and its properties will have a strong bearing on the nature of the potential-based target sets. For example, continuity and differentiability will lead to closed target sets since Definition 2.3 also stipulates that each  $\rho$  be in  $C_L^1$ . Under certain conditions it can even be shown that  $\mathbb{T}_\rho^f$  is a connected set in which case we can derive simple membership circuits; e.g., for boxes or bounded convex polytopes. This implies that it may often be practical and feasible to choose a target set that we know ex ante is a member of the (efficient) sub-algebra  $\tilde{\mathbb{T}}_\rho^f$ .

A counterfactual search problem that is expressible using potential duality can always be recast as an optimisation problem, where the goal is to find one or more points in a given counterfactual set  $\mathcal{S}_\rho^\varepsilon$ . Note, however, that Equation 4 defines the target set under a global sense of optimality, whereas existing gradient-based methods [55, 38] only find locally optimal solutions. Such methods find a CF as the limit point of a sequence  $\{x_n\}_{n \in \mathbb{N}_+}$  defined by a recurrence relation of the form:

$$x_{n+1} \leftarrow \Pi_{\mathcal{X}}[x_n + \eta \nabla \rho(f(x_n))] = \Pi_{\mathcal{X}}[x_n + \eta \rho'(f(x_n))^\top f'(x_n)], \quad (6)$$

where  $\Pi_{\mathcal{X}}$  denotes an Euclidean projection onto  $\mathcal{X}$ , and thus cannot apply to nondifferentiable models like boosted decision trees. Furthermore, gradient-based methods can fail with high probability, even if  $\nabla f$  exists [22]. Nevertheless, we show below that finding a CF using Equation 6 is CLS-complete while finding a globally optimal CF is CLS-hard. These complexity results complement those of Tsirtsis and Gomez Rodriguez [51] and also suggest that any instance of CFX-POTENTIAL-LOCALOPT can be transformed in polynomial time into problems such as GD-FINITE-DIFF [18]. This affords us access to a powerful toolbox of methods from numerical computing and optimisation.

**CFX-POTENTIAL-(LOCALOPT/GLOBALOPT) (informal)**

**Input:** A differentiable model  $f : \mathbb{R}^n \rightarrow \mathbb{R}^m$  and potential function  $\rho \in \mathcal{R}_q^f$ .

**Goal (LOCALOPT):** Find a point  $c \in \mathcal{X}$  such that  $\|c - \Pi_{\mathcal{X}}[c + \eta \nabla \rho(f(c))]\|_2 \leq \delta$ .

**Goal (GLOBALOPT):** Find an element of the counterfactual set  $\mathcal{S}_\rho^0$ .

---

**Theorem 2.2.** CFX-POTENTIAL-LOCALOPT is CLS-complete.

*Proof (Sketch).* Show inclusion by reducing to GENERAL-CONTINUOUS-LOCALOPT, then hardness follows by reducing from GD-LOCAL-SEARCH [18]; see Appendix A. □

**Corollary 2.2.1.** CFX-POTENTIAL-GLOBALOPT is CLS-hard.

*Proof (Sketch).* Follows directly from the injective mapping between solutions of CFX-POTENTIAL-GLOBALOPT and CFX-POTENTIAL-LOCALOPT; see Appendix A. □

## The Exponential-Polynomial Family

Potentials should facilitate CFs that are neither too near nor too far from the query, to ensure that CFs are both interpretable and actionable [52, 39]. To this end, we introduce the exponential-polynomial (EP) family of potentials in Definition 2.5 below that have this “sweet spot” property.

**Definition 2.5** (EP Family). For a model-query pair  $(f, q)$ , define the asymmetric exponential-polynomial (AEP) potentials as the functions

$$\rho_q^{\text{AEP}\pm}(y; w) \doteq z_q(y; w)_\pm^2 \exp\left\{-z_q(y; w)_\pm^2\right\}, \quad (7)$$

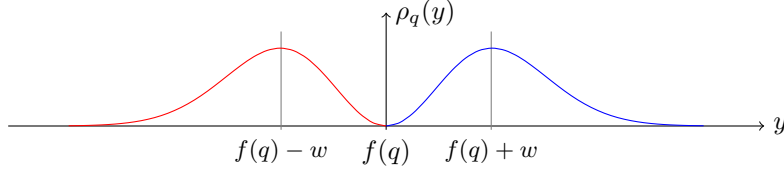


Figure 2: EP potential functions for query  $q$ , with  $\rho_q^{\text{AEP-}}$  and  $\rho_q^{\text{AEP+}}$  in red and blue, respectively.

whose arguments are the real value  $y \in \mathcal{Y} \subseteq \mathbb{R}$  and width parameter  $w > 0$ , with  $z_q(y; w) \doteq \frac{y-f(q)}{w}$ ,  $[z]_+ \doteq \max\{z, 0\}$ ,  $[z]_- \doteq -\min\{z, 0\}$ . The corresponding symmetric EP (SEP) potential is then

$$\rho_q^{\text{SEP}}(y; w) = \rho_q^{\text{AEP+}}(y; w) + \rho_q^{\text{AEP-}}(y; w). \quad (8)$$

By construction, EP potentials have customisable optima, and their shapes define nesting superlevel sets<sup>1</sup> which ensure consistent ordering of CFs. Figure 2 provides an example of EP potentials with maxima at  $f(q) \pm w$ , where the signs correspond to those in Definition 2.5.

### 3 Bayesian Optimisation and the EI-CFX Algorithm

Unlike existing work [55, 38, 14], we take a global optimisation perspective on the problem of finding CFEs by leveraging *Bayesian optimisation* [36, 24, 46], a technique that is sample-efficient and has known convergence guarantees. BO can be applied to non-differentiable models as it searches over the posterior distribution of a Gaussian process (GP) surrogate, and is thus applicable to models outside CFX-POTENTIAL-GLOBALOPT, like decision trees. However, as we show in Section 4, taking a naïve approach to using BO in this setting can lead to very poor performance. This can be attributed to the following question: should the surrogate just predict  $f$  or the entire composition  $\rho \circ f$ ? We argue that the former is better [3], since it makes our algorithm more effective and parallelisable by leveraging structure in the potential.

Suppose we have a model  $f$  that is continuous over  $\mathbb{R}$  and have sampled  $f(0) = 0$  and  $f(1) = 2$  under a potential  $\rho(y) = y^2 e^{-y^2}$ , yielding  $\rho(0) = 0$  and  $\rho(2) = 4e^{-4}$ . The intermediate value theorem now implies that there exists some  $z \in (0, 1)$  with  $f(z) = 1$  such that  $(\rho \circ f)(z)$  attains its maximum value of  $e^{-1}$ . A surrogate that models the composition  $\rho \circ f$  will not be guaranteed to attain this maximum. Figure 3 shows corroborating numerical evidence from a simple experiment, searching for counterfactuals for a logistic regression model with two features. We formulate the CF search using two different Bayesian optimisation problems, (a) using the explicit form of our EP potential  $\rho$  and modeling  $f$  with the surrogate, and (b) modeling the composition  $\rho \circ f$  with the surrogate. The former shows rapid convergence to the target set (red line), with the acquisition function recovering the desired set with just 7 or 8 samples. In contrast, the acquisition function of (b) does not show any meaningful convergence even after 8 samples.

To formalise our proposed method as a Bayesian optimisation problem we first take a scalar regression model  $f : \mathcal{X} \rightarrow \mathbb{R}$  and define the surrogate  $\hat{f}$  as being drawn from a GP prior,  $\mathcal{GP}(\mu, K)$ , with mean function  $\mu : \mathcal{X} \rightarrow \mathbb{R}$  and covariance function  $K : \mathcal{X} \times \mathcal{X} \rightarrow \mathbb{R}$ . Given a dataset  $\mathcal{D}_n \doteq \{(x_i, f(x_i))\}_{i \in [n]}$  we can also compute the posterior distribution  $\mathcal{GP}(\mu_n, K_n)$ , where the conditioned mean and covariance functions,  $\mu_n : \mathcal{X} \rightarrow \mathbb{R}$  and  $K_n : \mathcal{X} \times \mathcal{X} \rightarrow \mathbb{R}$ , can be evaluated in closed form [44]. Our novel acquisition function for performing (potential-based) counterfactual search then follows by a refinement of the well-known expected improvement function [36, 24]. As shown in Proposition 3.1 and Figure 3, this function admits “well-behaved,” closed-form expressions for its value and derivative.

<sup>1</sup>The  $\varepsilon$ -optimal target sets form an annulus of outer radius  $w$  and fixed inner radius under the SEP potential.

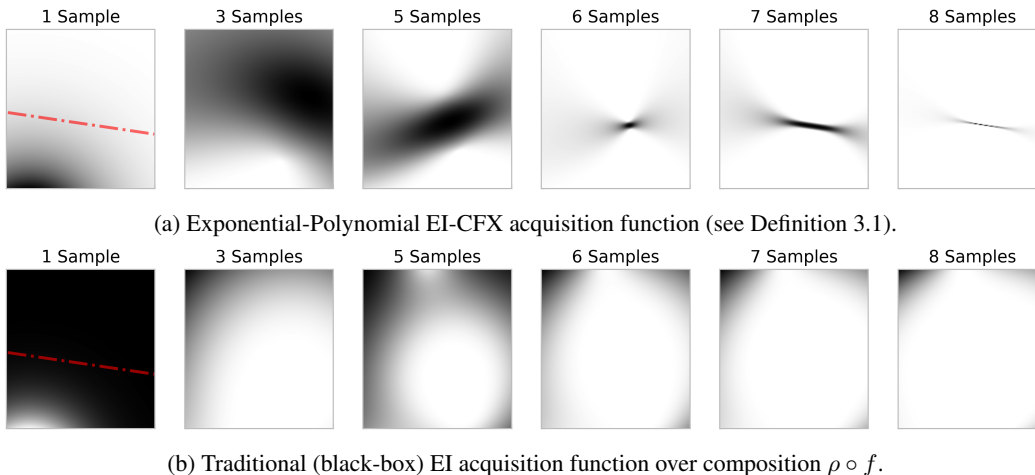


Figure 3: Acquisition function convergence for two features of a logistic regression model with EP potential and target of 50% probability; see Definition 2.5. The GP was conditioned on the same dataset in each row, darker pixels indicate higher values, and the red curve wraps the target set.

**Definition 3.1** (Expected Counterfactual Improvement). For a surrogate-potential pair  $(\hat{f}, \rho)$ , define the *expected counterfactual improvement* as

$$\begin{aligned} \text{EI-CFX}_n^\rho(x) &\doteq \mathbb{E}_n \left[ \max \left\{ 0, \rho \circ \hat{f}(x) - \rho_n^* \right\} \right] \\ &= \frac{1}{\sqrt{K_n(x)}} \int_{\mathbb{R}} \max \{ 0, \rho(y) - \rho_n^* \} \phi \left( \frac{y - \mu_n(x)}{\sqrt{K_n(x)}} \right) dy, \end{aligned} \quad (9)$$

where  $\mathbb{E}_n[X] \doteq \mathbb{E}[X | \mathcal{D}_n]$  is an expectation conditioned on a set of  $n$  samples  $\mathcal{D}_n \doteq \{(x_i, f(x_i))\}_{i \in [n]}$ ,  $\rho_n^* \doteq \max_i \{\rho(f(x_i)) : (x_i, f(x_i)) \in \mathcal{D}_n\}$  is the maximum potential observed over these samples, and  $\phi$  is the standard normal probability density function.

**Proposition 3.1.** *EI-CFX and  $\nabla \text{EI-CFX}$  are continuous functions of  $\mathcal{X}$  for any  $\rho \in \{\rho^{\text{AEP}^+}, \rho^{\text{AEP}^-}, \rho^{\text{SEP}}\}$  or  $n \geq 1$ .*

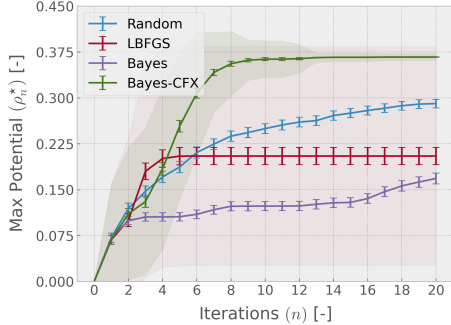
*Proof (Sketch).* Identify the 0-superlevel sets and replace the max operation with refined limits of integration. The rest follows through routine analysis of Gaussian integrals; see Appendix B.  $\square$

Under our composite structure of modeling just  $f$  with the surrogate, we can show that Bayesian optimisation using EI-CFX converges asymptotically to a globally optimal counterfactual. In other words, assuming that the counterfactual sets  $\mathcal{S}_\rho^\varepsilon$  are non-empty for all  $\varepsilon \geq 0$ , our proposed algorithm is guaranteed to find a point  $c \in \mathcal{S}_\rho^0$  in the limit of infinitely many observations,  $n \rightarrow \infty$ . This result, which we state informally below, establishes our algorithm as the first method for finding CFEs for regression models with global convergence guarantees. This proof holds even for non-differentiable models, which is a key advantage over past approaches [55, 38, 14], and motivates a wider adoption of Bayesian optimisation for solving instances of CFX-POTENTIAL-GLOBALOPT and related problems in this area.

**Theorem 3.2.** *The EI-CFX acquisition function is asymptotically consistent.*

*Proof (Sketch).* Follows directly from Theorem 1 of Astudillo and Frazier [3]; see Appendix C.  $\square$

Global convergence and improved use of information are not the only advantages of exploiting composition structure. With this approach, we are also able to generate multiple counterfactuals in a single pass by treating the search as a multi-objective problem [31, 14], as the  $n$ -sample dataset  $\mathcal{D}_n$  is entirely independent of the particular choice of potential. This contrasts with the alternative approach in which the potential is treated as part of the black-box, is modelled end-to-end by the surrogate, and leaves us with a set of samples that pertain only to a single counterfactual question. Here we can



(a) Average performance across all queries with the standard error of the mean. The shaded regions depict the standard deviation for L-BFGS-B and Bayes-CFX.

|                  | A           | CC            | HPW        |
|------------------|-------------|---------------|------------|
| Random           | 18.4        | -25270        | 10.9       |
| L-BFGS-B         | 15.3        | -1060         | 12.3       |
| Bayes            | 16.3        | 54590         | 10.2       |
| <b>Bayes-CFX</b> | <b>16.8</b> | <b>-24890</b> | <b>4.2</b> |

(b) Mean change to each feature across the counterfactuals generated for all queries for the features age (A), capital change (CC, the sum of capital gain and capital loss), and hours per week (HPW).

Figure 4: A summary of the counterfactual experiment results on the adult income dataset.

solve an arbitrary number of acquisition functions at each step and make use of the wider, shared dataset to bootstrap the search process, which can lead to improved convergence rates and fewer samples being needed.

## 4 Numerical Experiments

The objective of this section is to establish whether the theoretical arguments underpinning our Bayesian optimisation algorithm (and EI-CFX function) stand to account when applied in practice. To do this, we consider two well-known supervised learning problems based on: (a) the *adult income* dataset [17], for which we use a logistic regression model; and (b) the *New York City (NYC) taxi trip duration* dataset [25], for which we train a light gradient boosting machine (LightGBM) [28]. Details on hyperparameter selection and training are given in Appendix D. For all experiments, the GPyOpt [4] library was used for the Bayesian optimisation components, with the underlying GP furnished with an RBF kernel and zero mean function.

**Adult Income.** For the adult income dataset we posed the following broad question: “what would it take for the model to be class-indifferent, for young adults, given an initially confident classification?” To assess this, we took all inputs with an age less than 30 and at least 90% probability — as designated by the logistic regression model — of having a higher-income (i.e.  $f(q) \geq 0.9$ ). For each query instance  $q$ , we define the counterfactual potential  $\rho_q$  as the AEP<sup>-</sup> potential of Definition 2.5 with the width  $w$  set such that  $f(q) - w \doteq 0.5$ . The CF search problem is thus formulated as the optimisation  $\max_{x \in \mathcal{X}} \rho_q(f(x))$ . We then apply the following set of CF search algorithms and compare performance: (a) random search; (b) limited-memory Broyden–Fletcher–Goldfarb–Shanno quasi-Newton with bounds (L-BFGS-B) using box constraints [9, 58] and finite-difference gradients, to facilitate a comparison with the other gradient-free methods; (c) *Bayes*, where we optimise the composite function  $\rho_q(f(x))$  directly via Bayesian optimisation; and (d) *Bayes-CFX*, where we use the EI-CFX acquisition function of Definition 3.1 with Bayesian optimisation.

The results of this experiment, as illustrated in Figure 4, suggest that our proposed method is highly sample efficient and consistent across query instances and seeds. Panel (a) shows that Bayes-CFX converges after few queries to the highest potential value of the four methods. Panel (b) shows that Bayes-CFX incurs the smallest change in the hours-per-week feature (HPW) on average, with changes in the remaining features consistent with the other methods. The performance of L-BFGS-B was surprisingly poor, which could be due to convergence to a local optimum or limited memory preventing such convergence entirely [9]. Indeed, Bayes-CFX and random search both strongly support our thesis that performing gradient-based search directly on a surrogate modeling  $\rho \circ f$  is much less effective, even when the model  $f$  is differentiable. Note that random search, while certainly sub-optimal, was also able to achieve competitive performance across all cases, outperforming naïve Bayesian optimisation and L-BFGS-B.



Table 2: Sample set of counterfactuals generated using Bayes-CFX on the NYC taxi trip duration (LightGBM) model. In each case the target deviation and outcome is provided, the maximum number of features allowed to change under an  $\ell_0$  constraint, and the change in each feature. The query instance was for a one-person trip of 0.41 km that occurred on a Monday in May at 10AM.

| Target change | $\ell_0$ Bound | Change in  |                |              |               | Result change |
|---------------|----------------|------------|----------------|--------------|---------------|---------------|
|               |                | Passengers | Weekday [days] | Time [hours] | Distance [km] |               |
| +20%          | 1              | 0          | 0              | 0            | +2.16         | +19.6%        |
|               | 2              | 0          | +2             | 0            | +1.12         | +19.5%        |
|               | 3              | 0          | +1             | -1           | +1.18         | +19.9%        |
|               | 4              | +2         | -2             | +1           | +0.92         | +20.9%        |
| +10%          | 3              | 0          | 0              | 0            | -0.31         | +10.1%        |
| +50%          | 3              | 0          | +1             | -1           | +2.45         | +50.0%        |
| +100%         | 3              | +2         | +2             | 0            | +3.67         | +56.7%        |
|               | $\infty$       | +2         | +2             | +1           | +3.89         | +57.9%        |

**NYC Taxi Trip Durations.** For the NYC trip duration dataset we wanted to explore the impact of sparsity (via an  $\ell_0$  constraint) and satisfiability (via increasingly challenging targets) on the performance of the Bayes-CFX algorithm. To this end, we took a random query instance — modulo a constraint that the duration be in the lower tail of the distribution — and posed the following question: “what would it take to increase the trip duration by some fixed percentage?” We allowed the search method to increase the number of passengers by up to two, perturb the weekday and hour by unit increments in the range  $[-2, 2]$  and vary the distance by plus or minus one standard deviation about the query value. Example CFEs for a representative query instance — a one-person trip of 410m that occurred on a Monday in May at 10AM — are shown in Table 2.

The results suggest that distance is the leading factor of trip durations: it appears in all counterfactuals regardless of the sparsity constraint. We also found that the number of passengers played a consistent role when the target deviation was very large. These are both intuitive results as they align with the natural causal model of the problem; one cannot escape the laws of physics. Table 2 also highlights the value of counterfactuals for model diagnosis. For the counterfactual targeting a fare increase of +10%, we see that a substantial *decrease* in the distance was the only necessary change, which is unintuitive and could reflect traffic conditions, geographic locality or other confounding factors. Additionally, the counterfactuals that are earlier in the day (time -1 hr, i.e., 9 am) tend to be more expensive, which is understandable given that it is near the end of rush hour traffic. Furthermore, we see also that counterfactuals that are later in the day (time +1 hr, i.e., 11 am) correlates with more passengers, which could reflect a divide between business and social cab trips, particularly for weekend brunch (weekday -2 days and time +1 hour, i.e., Saturday at 11 am). Finally, we note that even when there is no constraint, there are some target deviations that were not possible to satisfy; this observation was also validated via brute-force computation. Nevertheless, by accumulating a dataset of candidate counterfactuals, the Bayes-CFX algorithm was able to yield a global “best-guess”. This is in contrast to existing (direct) gradient-based methods which are strictly local and path-dependent.

## 5 Conclusions and Future Directions

In this paper, the computational aspects of finding CFEs for regression models have been explored, the challenges around specification and formal robustness addressed, and a practical algorithm for solving such problems provided. This algorithm is shown to perform well in empirical experiments and is the first of its kind to enjoy global convergence guarantees (in the regression setting) — a result that holds even when the model itself is non-differentiable. We argue that this motivates wider use of Bayesian optimisation in this problem domain, and suggest that future work explore this direction further. As part of the research process, we have also contributed a principled mathematical framework that lays the foundations for rigorous theoretical studies into the algebraic and geometric properties of regression counterfactuals. In particular, we note that it would be possible — and indeed an interesting line of future work — to refine our counterfactual algebra to the set of *measurable* subsets in order to examine the probabilistic aspects of CFs. Moreover, it would also be of great

interest to investigate the impact of different classes of models on the  $\mathcal{S}$ - $\mathcal{T}$  duality. When the model is differentiable, for example, it is clear that potential-based target sets will comprise closed and connected sets. It stands to reason that a better understanding of this and other behaviours would yield more efficient, tailored search methods.

## Acknowledgments and Disclosure of Funding

The authors would like to acknowledge our colleague Nelson Vadori for their input during the analysis in Proposition 3.1.

**Disclaimer** This paper was prepared for informational purposes by the Artificial Intelligence Research group of JPMorgan Chase & Co and its affiliates (“J.P. Morgan”), and is not a product of the Research Department of J.P. Morgan. J.P. Morgan makes no representation and warranty whatsoever and disclaims all liability, for the completeness, accuracy or reliability of the information contained herein. This document is not intended as investment research or investment advice, or a recommendation, offer or solicitation for the purchase or sale of any security, financial instrument, financial product or service, or to be used in any way for evaluating the merits of participating in any transaction, and shall not constitute a solicitation under any jurisdiction or to any person, if such solicitation under such jurisdiction or to such person would be unlawful.

© 2021 JPMorgan Chase & Co. All rights reserved.

## References

- [1] André Artelt and Barbara Hammer. On the computation of counterfactual explanations – a survey. arXiv:1911.07749, 2019. URL <http://arxiv.org/abs/1911.07749>.
- [2] André Artelt and Barbara Hammer. Convex density constraints for computing plausible counterfactual explanations. In *Proc. of ICANN*, pages 353–365, 2020.
- [3] Raul Astudillo and Peter Frazier. Bayesian optimization of composite functions. In *Proc. of ICML*, pages 354–363, 2019.
- [4] The GPyOpt authors. GPyOpt: A Bayesian optimization framework in Python, 2016. URL <http://github.com/SheffieldML/GPyOpt>.
- [5] Solon Barocas, Andrew D. Selbst, and Manish Raghavan. The hidden assumptions behind counterfactual explanations and principal reasons. In *Proc. of FAccT*, pages 80–89, 2020.
- [6] J.S. Bergstra, D. Yamins, and D.D. Cox. Hyperopt: A Python library for optimizing the hyperparameters of machine learning algorithms. In *Proc. of SciPy*, pages 1–7, 01 2013.
- [7] Léon Bottou, Jonas Peters, Joaquin Quiñero-Candela, Denis X. Charles, D. Max Chickering, Elon Portugaly, Dipankar Ray, Patrice Simard, and Ed Snelson. Counterfactual reasoning and learning systems: The example of computational advertising. *JMLR*, 14:3207–3260, 2013.
- [8] Adam D. Bull. Convergence rates of efficient global optimization algorithms. *JMLR*, 12(88): 2879–2904, 2011.
- [9] Richard H. Byrd, Peihuang Lu, Jorge Nocedal, and Ciyou Zhu. A limited memory algorithm for bound constrained optimization. *SIAM J. Sci. Comput.*, 16(5):1190–1208, September 1995. ISSN 1064-8275. doi: 10.1137/0916069. URL <http://epubs.siam.org/doi/10.1137/0916069>.
- [10] Ruth M. J. Byrne. Counterfactual thought. *Ann. Rev. Psych.*, 67(1):135–157, 2016.
- [11] Jiahao Chen. Fair lending needs explainable models for responsible recommendation. In *FATREC Workshop on Responsible Recommendation*, 2018. URL <http://arxiv.org/abs/1809.04684>. arXiv:1809.04684.
- [12] Roberto Confalonieri, Ludovik Coba, Benedikt Wagner, and Tarek R. Besold. A historical perspective of explainable artificial intelligence. *Data Mining and Knowledge Discovery*, pages 1–21, 2020.

- [13] Robert M Corless, Gaston H Gonnet, David EG Hare, David J Jeffrey, and Donald E Knuth. On the Lambert- $W$  Function. *Advances in Computational Mathematics*, 5(1):329–359, 1996.
- [14] Susanne Dandl, Christoph Molnar, Martin Binder, and Bernd Bischl. Multi-objective counterfactual explanations. In *Proc. of the International Conference on Parallel Problem Solving from Nature*, pages 448–469. Springer, 2020.
- [15] Erik Daxberger, Anastasia Makarova, Matteo Turchetta, and Andreas Krause. Mixed-variable Bayesian optimization. In *Proc. of IJCAI*, pages 2633–2639, 7 2020.
- [16] Finale Doshi-Velez, Mason Kortz, Ryan Budish, Chris Bavitz, Sam Gershman, David O’Brien, Stuart Schieber, James Waldo, David Weinberger, and Alexandra Wood. Accountability of AI under the law: The role of explanation. arXiv:1711.01134, 2017. URL <http://arxiv.org/abs/1711.01134>.
- [17] Dheeru Dua and Casey Graff. UCI machine learning repository, 2017. URL <http://archive.ics.uci.edu/ml>.
- [18] John Fearnley, P Goldberg, Alexandros Hollender, and Rahul Savani. The complexity of gradient descent:  $CLS = PPAD \cap PLS$ . In *Proc. of STOC*, 2021.
- [19] Rubén R. Fernández, Isaac Martín de Diego, Víctor Aceña, Alberto Fernández-Isabel, and Javier M. Moguerza. Random forest explainability using counterfactual sets. *Information Fusion*, 63:196–207, 2020. ISSN 1566-2535.
- [20] Flyingwombat. Logistic Regression with UCI Adult Income, 2017. URL <https://www.kaggle.com/flyingwombat/logistic-regression-with-uci-adult-income>.
- [21] Steffen Grünewälder, Jean-Yves Audibert, Manfred Opper, and John Shawe-Taylor. Regret bounds for Gaussian process bandit problems. In *Proc. of AISTATS*, volume 9, pages 273–280, Chia Laguna Resort, Sardinia, Italy, May 2010.
- [22] Prateek Jain and Purushottam Kar. Non-convex optimization for machine learning. *Foundations and Trends in Machine Learning*, 10(3-4):142–336, 2017.
- [23] Eric Jang, Shixiang Gu, and Ben Poole. Categorical reparameterization with Gumbel-softmax. In *Proc. of ICLR*, page 12, 2017.
- [24] Donald R. Jones, Matthias Schonlau, and William J. Welch. Efficient global optimization of expensive black-box functions. *Global Optimization*, 13(4):455–492, 1998.
- [25] Kaggle. Playground prediction competition: New York City taxi trip duration, 2017. URL <https://www.kaggle.com/c/nyc-taxi-trip-duration>.
- [26] Kentaro Kanamori, Takuya Takagi, Ken Kobayashi, and Hiroki Arimura. Dace: Distribution-aware counterfactual explanation by mixed-integer linear optimization. In *Proc. of IJCAI*, pages 2855–2862, 2020.
- [27] Amir-Hossein Karimi, Bernhard Schölkopf, and Isabel Valera. Algorithmic recourse: From counterfactual explanations to interventions. In *Proc. of FAccT*, page 353–362, 2021.
- [28] Guolin Ke, Qi Meng, Thomas Finley, Taifeng Wang, Wei Chen, Weidong Ma, Qiwei Ye, and Tie-Yan Liu. LightGBM: A highly efficient gradient boosting decision tree. *Proc. of NeurIPS*, 30:3146–3154, 2017.
- [29] Arnaud Van Looveren and Janis Klaise. Interpretable counterfactual explanations guided by prototypes. arXiv:1907.02584, 2020. URL <https://arxiv.org/abs/1907.02584>.
- [30] Ana Lucic, Harrie Oosterhuis, Hinda Haned, and Maarten de Rijke. FOCUS: Flexible optimizable counterfactual explanations for tree ensembles, 2020.
- [31] Wenlong Lyu, Fan Yang, Changhao Yan, Dian Zhou, and Xuan Zeng. Batch bayesian optimization via multi-objective acquisition ensemble for automated analog circuit design. In *Proc. of ICML*, pages 3306–3314, 2018.

- [32] Chris J Maddison, Andriy Mnih, and Yee Whye Teh. The concrete distribution: A continuous relaxation of discrete random variables. In *Proc. of ICLR*, 2017.
- [33] Divyat Mahajan, Chenhao Tan, and Amit Sharma. Preserving causal constraints in counterfactual explanations for machine learning classifiers, 2020.
- [34] Kenneth L. Manders and Leonard Adleman. NP-complete decision problems for binary quadratics. *Computer and System Sciences*, 16(2):168–184, 1978.
- [35] Tim Miller. Explanation in artificial intelligence: Insights from the social sciences. *Artificial Intelligence*, 267:1–38, 2019.
- [36] J. Moćkus. On Bayesian methods for seeking the extremum. In *Optimization Techniques IFIP Technical Conference*, pages 400–404. Springer, Berlin Heidelberg, 1975.
- [37] Dov Monderer and Lloyd S Shapley. Potential games. *Games and Economic Behavior*, 14(1): 124–143, 1996.
- [38] Ramaravind K. Mothilal, Amit Sharma, and Chenhao Tan. Explaining machine learning classifiers through diverse counterfactual explanations. In *Proc. of FAccT*, pages 607–617, New York, NY, USA, January 2020. ACM. doi: 10.1145/3351095.3372850.
- [39] Martin Pawelczyk, Klaus Broelemann, and Gjergji Kasneci. On counterfactual explanations under predictive multiplicity. In *Proc. of UAI*, volume 124, pages 809–818, 2020.
- [40] Martin Pawelczyk, Klaus Broelemann, and Gjergji Kasneci. Learning model-agnostic counterfactual explanations for tabular data. In *Proc. of WWW*, page 3126–3132, 2020.
- [41] Judea Pearl. *Causality: Models, Reasoning and Inference*. Cambridge University Press, USA, 2nd edition, 2009.
- [42] Rafael Poyiadzi, Kacper Sokol, Raul Santos-Rodriguez, Tijl De Bie, and Peter Flach. FACE: Feasible and actionable counterfactual explanations. In *Proc. of AIES*, page 344–350, 2020.
- [43] Quentinmonmousseau. ML Workflow: LightGBM  $\approx$  0.37, RandomForest  $\approx$  0.39, 2019. URL <https://www.kaggle.com/quentinmonmousseau/ml-workflow-lightgbm-0-37-randomforest-0-39>.
- [44] Carl Edward Rasmussen and Christopher K. I. Williams. *Gaussian Processes for Machine Learning*. The MIT Press, 2005.
- [45] Binxin Ru, Ahsan Alvi, Vu Nguyen, Michael A. Osborne, and Stephen Roberts. Bayesian optimisation over multiple continuous and categorical inputs. In *Proc. of ICML*, volume 119, pages 8276–8285, 2020.
- [46] Bobak Shahriari, Kevin Swersky, Ziyu Wang, Ryan P. Adams, and Nando de Freitas. Taking the human out of the loop: A review of Bayesian optimization. *Proc. of IEEE*, 104(1):148–175, 2016.
- [47] Jasper Snoek, Hugo Larochelle, and Ryan P. Adams. Practical bayesian optimization of machine learning algorithms. In *Proc. of NeurIPS*, pages 2951–2959, 2012.
- [48] Niranjan Srinivas, Andreas Krause, Sham M. Kakade, and Matthias W. Seeger. Information-theoretic regret bounds for gaussian process optimization in the bandit setting. *IEEE Transactions on Information Theory*, 58:3250–3265, 2012.
- [49] Ilija Stepin, Jose M. Alonso, Alejandro Catala, and Martín Pereira-Fariña. A survey of contrastive and counterfactual explanation generation methods for explainable artificial intelligence. *IEEE Access*, 9:11974–12001, 2021.
- [50] Gabriele Tolomei, Fabrizio Silvestri, Andrew Haines, and Mounia Lalmas. Interpretable predictions of tree-based ensembles via actionable feature tweaking. In *Proc. of KDD*, page 465–474, 2017.

- [51] Stratis Tsirtsis and Manuel Gomez Rodriguez. Decisions, counterfactual explanations and strategic behavior. In H. Larochelle, M. Ranzato, R. Hadsell, M. F. Balcan, and H. Lin, editors, *Proc. of NeurIPS*, volume 33, pages 16749–16760. Curran Associates, Inc., 2020.
- [52] Berk Ustun, Alexander Spangher, and Yang Liu. Actionable recourse in linear classification. In *Proc. of FAccT*, page 10–19, 2019.
- [53] Sahil Verma, John Dickerson, and Keegan Hines. Counterfactual explanations for machine learning: A review. In *NeurIPS Workshop on Machine Learning Retrospectives, Surveys & Meta-Analyses*, 2020. URL <http://arxiv.org/abs/2010.10596>.
- [54] Paul Voigt and Axel Von dem Bussche. *The EU General Data Protection Regulation (GDPR): A Practical Guide*. Springer, 1 edition, 2017.
- [55] S Wachter, BDM Mittelstadt, and C Russell. Counterfactual explanations without opening the black box: Automated decisions and the gdpr. *Harvard Journal of Law and Technology*, 31: 841–887, 2018.
- [56] Yixin Wang and David M. Blei. The blessings of multiple causes. *J. Amer. Stat. Assoc.*, 114 (528):1574–1596, 2019.
- [57] Yichi Zhang, Daniel W. Apley, and Wei Chen. Bayesian optimization for materials design with mixed quantitative and qualitative variables. *Scientific Reports*, 10(1):4924, 2020.
- [58] Ciyou Zhu, Richard H. Byrd, Peihuang Lu, and Jorge Nocedal. Algorithm 778: L-BFGS-B: Fortran subroutines for large-scale bound-constrained optimization. *ACM Trans. Math. Softw.*, 23(4):550—560, December 1997.

## A Complexity Results

In this section we outline our proofs for the complexity results included in the paper. We will restrict our attention only to *well-behaved* circuits that may be evaluated in polynomial-time with respect to their input and output spaces. In particular, we leverage the definition of Fearnley et al. [18] which states that an arithmetic circuit is well-behaved if, on any directed path that leads to an output, there are at most  $\log(\text{size}(f))$  *true* multiplication gates. A true multiplication gate is one where both inputs are non-constant nodes of the circuit. Even allowing an unrestricted number of constant multiplications, it can be shown that (a) we can check that a given arithmetic circuit is well-behaved in polynomial time; and (b) that such a circuit may be evaluated efficiently. For a proof of this claim we refer the reader to Lemma 3.3 of Fearnley et al. [18] and their subsequent discussion on the robustness of this formulation.

### A.1 CFX-EXISTENCE

The first problem that was presented in the paper asks the question of whether the primal space associated with a model-query-target set triple  $(f, q, \mathcal{T}_q)$  is or isn't non-empty. Note that since  $\mathcal{T}_q \in \mathbb{T}_q$ , by construction we have that all elements in the dual space are reachable, but we do not know whether the corresponding primal space  $\mathcal{S}_q$  has entries (see Definition 2.2). For example, if the model output  $f(q)$  is only achieved at the query point itself, then by definition there is no set in the algebra  $\mathbb{T}_q$  such that the primal is non-empty. Of course, we do not know this ex ante, and finding a solution may require enumeration of all sets in the algebra in the worst case! On the other hand, taking any query  $q \in \mathcal{X}$ , we can always choose an empty dual space  $\emptyset \in \mathbb{T}_q$  for which the assertion is satisfied immediately. As we show below, this problem can be shown to be NP-complete. To do so, we first define a *membership circuit* which is used to constrain the model domain in a principled way; recall that the existence of such a circuit is the defining property of a target set  $\mathcal{T}$  that is an element of the efficient sub-algebra  $\tilde{\mathbb{T}}_q$ .

**Definition A.1** (Membership Circuit). Let  $\mathcal{A}$  be an arbitrary topological space. A *membership circuit*,  $M_{\mathcal{T}} : \mathcal{A} \rightarrow \{0, 1\}$ , with respect to a subset  $\mathcal{T} \subseteq \mathcal{A}$  is then defined such that

$$M_{\mathcal{T}}(a) = \begin{cases} 1 & \text{if } a \in \mathcal{T}, \\ 0 & \text{otherwise.} \end{cases} \quad (10)$$

**CFX-EXISTENCE**

**Input:**

- A well-behaved arithmetic (model) circuit  $f : \mathcal{X} \rightarrow \mathcal{Y}$ ,
- query instance  $q \in \mathcal{X}$ ,
- and dual set  $\mathcal{T} \in \tilde{\mathbb{T}}_q^f$  with well-behaved membership circuit  $M_{\mathcal{T}}$ .

**Goal:** Decide if the counterfactual (primal) set  $\mathcal{S}$  is non-empty.

**Theorem 2.1.** CFX-EXISTENCE is NP-complete.

*Proof.* We prove completeness by first showing that CFX-EXISTENCE admits polynomial-time solution verification, and then identifying a reduction from SAT which implies hardness.

**Inclusion.** We demonstrate a certificate of polynomial length that may be verified in polynomial time. Note that any proposed counterfactual point  $c \in \mathcal{X}$  acts as a witness to verify that  $\mathcal{S}$  is non-empty. The certificate requirement is thus satisfied by construction since  $\mathcal{X}$  is finite dimensional. Then, since the assertion that  $f(c) \in \mathcal{T}$  may be computed in polynomial-time using the membership circuit, it follows that we have recovered the verifier definition of NP.

**Hardness.** We reduce from SAT. Let  $\phi : \mathcal{X} \rightarrow \{0, 1\}$  denote a boolean formula which evaluates to TRUE (i.e. 1) iff  $f(x) \in \mathcal{T}$ , and FALSE (i.e. 0) otherwise; note that this operation can be performed in polynomial-time using the membership circuit. If the set  $\mathcal{T}_q$  is empty then the formula  $\phi$  is unsatisfiable, whence deciding if  $\mathcal{S}$  is empty or not is NP-hard.  $\square$

## A.2 CFX-POTENTIAL-LOCALOPT

The second problem presented in the paper was concerned with *finding* a counterfactual point that is locally optimal with respect to a given potential. The definition, which we state formally below, is closely related to the GD-LOCAL-SEARCH problem of Fearnley et al. [18]. In particular, CFX-POTENTIAL-LOCALOPT can be seen as a constrained variant in which we stipulate a promise that the function  $\rho$  is a valid counterfactual potential; i.e. does not attain a global optimum at the query instance. In general, establishing whether this promise is held is hard since it amounts to a global optimisation problem in and of itself. As such, we rely on an explicit promise since it is unclear how one might define an efficient violation witness.<sup>2</sup> As we show in Theorem 2.2 below, this does not change the complexity of the problem since the solution criterion is otherwise unchanged, though we acknowledge that this renders the reduction slightly less natural. Overall, the conclusions align with the results of Fearnley et al. [18], which suggest that the class CLS is robust to promise variants of the otherwise complete (total) problems considered.

**CFX-POTENTIAL-LOCALOPT**

**Input:**

- Bounded non-empty domain  $\mathcal{X} = \{x \in \mathbb{R}^n : Ax \leq b\}$  for  $(A, b) \in \mathbb{R}^{m \times n} \times \mathbb{R}^m$ ,
- well-behaved arithmetic (model) circuits  $f : \mathbb{R}^n \rightarrow \mathbb{R}^d$  and  $\nabla f : \mathbb{R}^n \rightarrow \mathbb{R}^{d \times n}$ ,
- well-behaved arithmetic (potential) circuits  $\rho : \mathbb{R}^d \rightarrow \mathbb{R}$  and  $\nabla \rho : \mathbb{R}^d \rightarrow \mathbb{R}^d$ ,
- Lipschitz constant  $L > 0$ , step size  $\eta > 0$ , and tolerance  $\delta > 0$ .

**Promise:** The model circuit  $\rho$  is a valid counterfactual potential (see Definition 2.3).

**Goal:** Find a point  $c \in \mathcal{X}$  such that  $\|c - \Pi_{\mathcal{X}}[c + \eta \nabla \rho(f(c))]\|_2 \leq \delta$ .

Alternatively, we accept one of the following violation cases as a solution:

- One of  $f, \nabla f, \rho$  or  $\nabla \rho$  is not  $L$ -Lipschitz.
- $\nabla f$  is not the gradient of  $f$ .
- $\nabla \rho$  is not the gradient of  $\rho$ .

**Theorem 2.2.** CFX-POTENTIAL-LOCALOPT is CLS-complete.

*Proof.* We prove completeness by first showing inclusion in CLS, and then identifying a reduction from GD-LOCAL-SEARCH which implies hardness.

**Inclusion.** Observe that CFX-POTENTIAL-LOCALOPT reduces immediately to GENERAL-CONTINUOUS-LOCALOPT by instantiating  $p(x) \doteq (\rho \circ f)(x)$  and  $g(x) \doteq x + \eta \nabla [\rho(f(x))]$ , where the gradient  $\nabla [\rho(f(x))] = [\nabla \rho](f(x))^\top [\nabla f](x)$  follows from the chain rule. These quantities can be computed in polynomial-time since the operations comprise only of well-behaved arithmetic circuits and an  $(1 \times d)$ -by- $(d \times n)$  vector-matrix product, where  $d, n < \infty$ . As shown by Fearnley et al. [18] in Proposition 5.6, this implies inclusion in CLS. Furthermore, this result holds regardless of whether the potential promise is kept or not, since the remaining violation conditions are identical in both problems, and GENERAL-CONTINUOUS-LOCALOPT otherwise has the same solution set.

**Hardness.** To show hardness, we need only prove that GD-LOCAL-SEARCH over the domain  $\mathcal{X} \doteq [0, 1]^2$  can be reduced to CFX-POTENTIAL-LOCALOPT; see Theorem 5.1 of Fearnley et al. [18]. For this, consider an instance of GD-LOCAL-SEARCH,  $(\delta, \eta, g, \nabla g, L)$ , where the objective is to find a stationary point of  $g$ . In order to reduce to CFX-POTENTIAL-LOCALOPT, we must identify an instance  $(\delta, \eta, f, \nabla f, \rho, \nabla \rho, L)$  in which there is equivalence in solutions; i.e. an algorithm for solving CFX-POTENTIAL-LOCALOPT can also be used to solve GD-LOCAL-SEARCH. This can be achieved by instantiating the potential as  $\rho(y) \doteq y$  such that  $\nabla \rho(y) = 1$ , and model function as  $f(x) \doteq -g(x)$  such that  $\nabla f = -\nabla g$ . This is promise-breaking in the sense that  $\rho$  is not guaranteed to be a valid potential for any given  $f$ . However, the solutions to CFX-POTENTIAL-LOCALOPT are

<sup>2</sup>Note that, if we could design such a witness, a violation solution would also satisfy the requirements for our hardness reduction.

all valid for GD-LOCAL-SEARCH even if the promise was indeed broken. With this construction we ensure that the Lipschitz constant is unchanged between the two problem instances, and thus the violation solutions are immediately preserved. We thus have a polynomial-time reduction and the proof is complete.  $\square$

### A.3 CFX-POTENTIAL-GLOBALOPT

**CFX-POTENTIAL-GLOBALOPT**

**Input:**

- Bounded non-empty domain  $\mathcal{X} = \{x \in \mathbb{R}^n : Ax \leq b\}$  for  $(A, b) \in \mathbb{R}^{m \times n} \times \mathbb{R}^m$ ,
- well-behaved arithmetic (model) circuits  $f : \mathbb{R}^n \rightarrow \mathbb{R}^d$  and  $\nabla f : \mathbb{R}^n \rightarrow \mathbb{R}^{d \times n}$ ,
- well-behaved arithmetic (potential) circuits  $\rho : \mathbb{R}^d \rightarrow \mathbb{R}$  and  $\nabla \rho : \mathbb{R}^d \rightarrow \mathbb{R}^d$ ,
- Lipschitz constant  $L > 0$  and tolerance  $\varepsilon > 0$ .

**Promise:** The model circuit  $\rho$  is a valid counterfactual (see Definition 2.3).

**Goal:** Find an element of the counterfactual set  $\mathcal{S}_\rho^\varepsilon$ .

Alternatively, we accept one of the following violation cases as a solution:

- One of  $f$ ,  $\nabla f$ ,  $\rho$  or  $\nabla \rho$  is not  $L$ -Lipschitz.
- $\nabla f$  is not the gradient of  $f$ .
- $\nabla \rho$  is not the gradient of  $\rho$ .

**Corollary 2.2.1.** CFX-POTENTIAL-GLOBALOPT is *CLS-hard*.

*Proof.* The proof follows using the same logic as that for Theorem 2.2, but instantiating CFX-POTENTIAL-GLOBALOPT with the tolerance  $\varepsilon \doteq 0$ . This ensures that the only solutions are globally optimal points which will also be valid for GD-LOCAL-SEARCH since the gradient at any of the corresponding inputs must be zero. This concludes the proof.  $\square$

## B EI-CFX Acquisition Function

In this section we will go over the proof of Proposition 3.1 and examine the derivation of the closed-form expression for the EI-CFX acquisition function. Recall that, for a given model-potential pair  $(f, \rho)$ , the EI-CFX function is given by the Gaussian integral

$$\text{EI-CFX}_n^\rho(x) = \frac{1}{\sqrt{K_n(x)}} \int_{\mathbb{R}} \max\{0, \rho(y) - \rho_n^*\} \phi\left(\frac{y - \mu_n(x)}{\sqrt{K_n(x)}}\right) dy.$$

As will be shown below, this function can be evaluated efficiently and resolves to a continuous function with (relatively) well-behaved derivative.

**Proposition 3.1.** *EI-CFX and  $\nabla \text{EI-CFX}$  are continuous functions of  $\mathcal{X}$  for any  $\rho \in \{\rho^{\text{AEP}^+}, \rho^{\text{AEP}^-}, \rho^{\text{SEP}}\}$  or  $n \geq 1$ .*

*Proof.* For clarity of exposition, fix the iteration number  $n \geq 1$ , take the symmetric EP potential  $\rho^{\text{SEP}}$  for a query  $q \in \mathcal{X}$ , and define the shorthand notation  $\alpha(x) \doteq \text{EI-CFX}_n^\rho(x)$ . We will show that the analysis for  $\rho^{\text{SEP}}$  generalises that of  $\rho^{\text{AEP}^\pm}$  and is independent of the particular value of  $n$ .

To begin, we perform a change of measure such that  $\alpha(x)$  is expressed in terms of the standard Normal distribution:

$$\alpha(x) = \int_{\mathbb{R}} \max\{0, \rho_q(\mu_x + \sigma_x z) - \rho_n^*\} \phi(z) dz, \quad (11)$$

where  $\phi(\cdot)$  is the PDF of the standard Normal distribution with  $y \doteq \mu_x + \sigma_x z$  and  $z \sim \mathcal{N}(0, 1)$ . The mean and standard deviation of the GP after the  $n$  iterations have also been simplified to  $\mu_x \doteq \mu_n(x)$  and  $\sigma_x \doteq \sqrt{K_n(x, x)}$ , respectively.



Now, to remove the max non-linearity observe that, for  $0 < \rho_n^* \leq 1/e$ , the SEP potential has exactly four real roots. Further, when  $\rho_n^* = 1/e$ , these four values degenerate to two unique solutions that are also minima of the function. This means that we can replace the max operation with limits of integration that restrict the summation only to the positive parts. To formalise this, we provide the following auxiliary lemma:

**Lemma B.1.** *Let  $c \in [-1/e, 0)$  denote a constant, then the four real solutions to the equation  $-x^2 e^{-x^2} = c$  are given by  $x = \pm i\sqrt{W_{-1}(c)}$  and  $x = \pm i\sqrt{W_0(c)}$ , where  $W_k(x)$  denotes the  $k^{\text{th}}$  branch of Lambert's  $W$ -function [13]. When  $c = -1/e$ , then  $W_{-1}(c) = W_0(c)$  and the two remaining solutions are  $x = \pm i\sqrt{W_{-1}(c)}$ .*

*Proof.* The original equation implies that  $-x^2 = W_k(c)$  for any  $k \in \mathbb{Z}$ , and thus that  $x = \pm i\sqrt{W_k(c)}$ . Since the only real branches of Lambert's  $W$ -function are for  $k \in \{-1, 0\}$ , the only real solutions must have the form stated in the claim. The degeneracy then follows from the fact that the principal branch is separated from the  $k = \pm 1$  branches by a cut at  $c = 1/e$  [13].  $\square$

Lemma B.1 above implies that  $\alpha(\cdot)$  may be decomposed into the following two integrals:

$$\alpha(x) = \underbrace{\int_{\tau_0^+}^{\tau_{-1}^+} [\rho(\mu_x + \sigma_x z) - \rho_n^*] \phi(z) dz}_{\alpha^+(x)} + \underbrace{\int_{\tau_{-1}^-}^{\tau_0^-} [\rho(\mu_x + \sigma_x z) - \rho^*] \phi(z) dz}_{\alpha^-(x)}, \quad (12)$$

where

$$\tau_k^\pm \doteq \frac{\pm iw\sqrt{W_k(\rho_n^*)} - \tilde{\mu}_x}{\sigma_x}, \quad (13)$$

and  $\tilde{\mu}_x \doteq \mu_x - \rho(q)$ . The functions  $\alpha^\pm(\cdot)$  have the natural interpretation of being the (re-scaled) expected counterfactual improvement with respect to the potential under negative/positive perturbations. They also correspond to applying a Gaussian kernel over the two regions for which  $\rho_q(\mu_x + \sigma_x z) - \rho_q^*$  is in either of the two positive quadrants, as illustrated in Figure 2.

Focusing only on the positive case (the negative follows analogously) we can show that

$$\begin{aligned} \alpha^+(x) &= \rho_n^* [\Phi(\tau_0^+) - \Phi(\tau_{-1}^+)] + \int_{\tau_0^+}^{\tau_{-1}^+} \rho_q(\mu_x + \sigma_x z) \phi(z) dz, \\ &= \rho_n^* [\Phi(\tau_0^+) - \Phi(\tau_{-1}^+)] + \underbrace{\frac{1}{w^2} \int_{\tau_0^+}^{\tau_{-1}^+} [\tilde{\mu}_x + \sigma_x z]^2 \exp\left\{-\left[\frac{\tilde{\mu}_x + \sigma_x z}{w}\right]^2\right\} \phi(z) dz}_{I^+(x)}, \end{aligned}$$

where  $\Phi(\cdot)$  denotes the standard Normal CDF. One may then solve the remaining integral by substitution, taking<sup>3</sup>

$$\kappa \doteq w^2 + 2\sigma_x^2, \quad a \doteq \frac{2\tilde{\mu}_x^2}{\kappa}, \quad b \doteq \frac{2\tilde{\mu}_x\sigma_x}{\kappa},$$

such that the exponent reduces in the following way:

$$\begin{aligned} -\frac{\tilde{\mu}_x^2 + 2\tilde{\mu}_x\sigma_x z + \sigma_x^2 z^2}{w^2} - \frac{z^2}{2} &= -\frac{1}{2w^2} [2\tilde{\mu}_x^2 + 4\tilde{\mu}_x\sigma_x z + (2\sigma_x^2 + w^2) z^2], \\ &= -\frac{\kappa}{2w^2} [a + 2bz + z^2], \\ &= -\frac{\kappa}{2w^2} [(b+z)^2 + a - b^2]. \end{aligned}$$

This means that the exponential term in  $\alpha^+(\cdot)$  can be expressed as

$$\underbrace{\exp\left\{\frac{\kappa}{2w^2} (b^2 - a)\right\}}_{\text{Constant}} \underbrace{\exp\left\{-\frac{\zeta^2}{2}\right\}}_{\text{Integrand}},$$

<sup>3</sup>Note that we drop subscripts denoting dependence for notational clarity. It should be assumed that everything depends on the input argument  $x$ .

via a second change of variables, with  $\zeta \doteq \sqrt{\frac{\kappa}{w^2}}(b+z)$ . This is convenient because we have now isolated the integrand — it remains only to evaluate a standard Gaussian integral.

Taking  $d\zeta = \sqrt{\frac{\kappa}{w^2}} dz$  and  $z = \sqrt{\frac{w^2}{\kappa}} \zeta - b$ , we arrive at the transformed integral

$$I^+ = C \int_{\tau_0'^+}^{\tau_{-1}'^+} \left[ \tilde{\mu}_x - b\sigma_x + \sqrt{\frac{w^2}{\kappa}} \sigma_x \zeta \right]^2 \phi(\zeta) d\zeta,$$

where  $\tau_n'^{\pm} \doteq \sqrt{\frac{\kappa}{w^2}}(b + \tau_n^{\pm})$  and  $C \doteq \exp\left\{\frac{\kappa}{2w^2}(b^2 - a)\right\} \sqrt{\frac{1}{w^2\kappa}}$ . This integral can then be broken down into three terms as follows:

$$\begin{aligned} \frac{1}{C} I^+(x) &= \int_{\tau_0'^+}^{\tau_{-1}'^+} \left[ \tilde{\mu}_x - b\sigma_x + \sqrt{\frac{w^2}{\kappa}} \sigma_x \zeta \right]^2 \phi(\zeta) d\zeta, \\ &= [\tilde{\mu}_x - b\sigma_x]^2 \int_{\tau_0'^+}^{\tau_{-1}'^+} \phi(\zeta) d\zeta \\ &\quad + 2\sqrt{\frac{w^2}{\kappa}} \sigma_x [\tilde{\mu}_x - b\sigma_x] \int_{\tau_0'^+}^{\tau_{-1}'^+} \zeta \phi(\zeta) d\zeta \\ &\quad + \frac{w^2 \sigma_x^2}{\kappa} \int_{\tau_0'^+}^{\tau_{-1}'^+} \zeta^2 \phi(\zeta) d\zeta, \end{aligned}$$

where the right hand side resolves to

$$\left[ \left[ (\tilde{\mu}_x - b\sigma_x)^2 + \frac{w^2 \sigma_x^2}{\kappa} \right] \Phi(\zeta) - 2\sqrt{\frac{w^2}{\kappa}} \sigma_x [\tilde{\mu}_x - b\sigma_x] \phi(\zeta) - \frac{w^2 \sigma_x^2}{\kappa} \zeta \phi(\zeta) \right]_{\tau_0'^+}^{\tau_{-1}'^+}.$$

To simplify further, we can define  $\gamma \doteq \tilde{\mu}_x - b\sigma_x$  and  $\eta \doteq \frac{w\sigma_x}{\sqrt{\kappa}}$  such that

$$I^+(x) = C \left[ (\gamma^2 + \eta^2) \Phi(\zeta) - 2\eta\gamma\phi(\zeta) - \eta^2\zeta\phi(\zeta) \right]_{\tau_0'^+}^{\tau_{-1}'^+},$$

with the same logic implying that

$$I^-(x) = C \left[ (\gamma^2 + \eta^2) \Phi(\zeta) - 2\eta\gamma\phi(\zeta) - \eta^2\zeta\phi(\zeta) \right]_{\tau_{-1}'^-}^{\tau_0'^-}.$$

These functions are both continuous in the argument  $x$  and the derivative follows from the product rule, standard Gaussian identities and properties of Lambert's  $W$ -function [13] to give a closed-form expression.<sup>4</sup> Substituting back into  $\alpha^{\pm}(x)$  we clearly maintain continuity. Finally, note that (a) the value of  $n$  doesn't affect the result; and (b) that the decomposition in Equation 12 aligns exactly with the distinctions between the SEP and AEP $^{\pm}$  potentials. It follows that the continuity property holds for all three potentials and thus the proof is complete.  $\square$

## C Asymptotic Consistency and Global Optimality

In this final section we include a formal statement of the global convergence guarantee of our Bayesian optimisation algorithm. In particular, we show below that this result follows directly from the result proved by Theorem 1 of Astudillo and Frazier [3].

**Theorem 3.2.** *Let  $\{x_n\}_{n \in \mathbb{N}}$  denote a sequence of points generated by the optimisation routine such that, for some  $n_0 \in \mathbb{N}$  and all  $n \geq n_0$ , the iterates satisfy the inclusion relation*

$$x_{n+1} \in \arg \max_{x \in \mathcal{X}} EI\text{-CFX}_n(x).$$

*Then, under suitable regularity conditions, and as  $n \rightarrow \infty$ , we have that*

$$\rho_n^* \rightarrow \rho^* = \max_{x \in \mathcal{X}} \rho(f(x)).$$

<sup>4</sup>We omit the explicit derivation of this expression as it's not particularly constructive. We simply note that while we implemented this exactly, one can use any robust autograd library to perform the computation with ease.

*Proof.* The proof follows directly from Theorem 1 of Astudillo and Frazier [3] under the assumption that the covariance function of the GP satisfies the Generalised-No-Empty-Ball property (Definition 5.1 in [3]). This can be seen by direct instantiation of their functions  $g(y)$  and  $f(x)$  with the potential and model functions, respectively.  $\square$

## D Model Training

### D.1 Adult Income

The adult-income model comprised two stages — a preprocessing phase and a model fitting phase — that followed an example from the kaggle website [20]. We outline the two parts below.

#### Preprocessing.

1. Compress the “Workclass” feature such that:
  - (a) “Without-pay” and “Never-worked” is merged into “Unemployed.”
  - (b) “State-gov” and “Local-gov” is merged into “Government.”
  - (c) “Self-emp-inc” and “Self-emp-not-inc” were merged into “Self-employed”.
2. Compress the “Marital Status” feature such that “Married-AF-spouse,” “Married-civ-spouse,” and “Married-spouse-absent” were merged into one value “Married.”
3. Group the “Country” feature into the following categories:
  - (a) “North America”
  - (b) “Asia”
  - (c) “South America”
  - (d) “Europe”
  - (e) “Other,” which includes the spurious values “South” and “?”.
4. Remove all rows that contain missing values; i.e. “?” values.
5. Apply a standard scaling to the numerical features.
6. Apply an ordinal encoding to the ordinal features.
7. Apply a one-hot encoding to the categorical features.

**Fitting.** The logistic regression model was then fit using an 80/20 training/testing data-split using a randomly initialised random state of 7. An  $\ell_2$  regulariser was added with unit scaling. The resulting accuracy was measured at approximately 85% on the holdout dataset.

### D.2 NYC Taxi Trip Duration

As with the adult-income model, the model development for the NYC Taxi dataset comprised two stages — preprocessing phase and model fitting — that followed an example from the kaggle website [43]. We outline the two parts below.

#### Preprocessing.

1. Filter the dataset for sensible values:
  - (a) A “trip\_duration” of less than 5900.
  - (b) A non-zero “passenger\_count.”
  - (c) A “pickup\_longitude” of greater than -100 and “pickup\_latitude” of less than 50.
2. Apply a log transformation to the “trip\_duration” feature to make the distribution “more Normal”.
3. Apply one-hot encodings to the “store\_and\_fwd\_flag” and “vendor\_id” features.
4. Drop the “dropoff\_datetime” column.
5. Split the “pickup\_datetime” column into months, weeks, weekdays, hours and minutes of the day features, dropping the original column.

6. Add Haversine distance and direction features based on the pickup and dropoff locations, and filter by those rows with “distance” less than 200.
7. Compute the implied speed of the taxi and filter by those values where the new “speed” features was less than 30.

**Fitting.** A light gradient-boosting machine model was fit on the training dataset using: a learning rate of 0.1; maximum depth of 25; 1000 leaves; feature fraction of 0.9; bagging fraction of 0.5; and a maximum bin of 1000. A random seed of 123 was used during training.